4572 *Chem. Mater.* **2010,** *22,* 4572–4578
DOI:10.1021/cm100486r

CHEMISTRY OF MATERIALS
Article

Structure, Microstructure, and Microwave Dielectric Properties of $(Sr_{2-x}Ca_x)(MgTe)O_6$ Double Perovskites

Rick Ubic,*,† Steven Letourneau,† Sherin Thomas,‡ G. Subodh,§ and M. T. Sebastian‡

†*Department of Materials Science & Engineering, Boise State University, 1910 University Drive, Boise, Idaho 83725,* ‡*Materials and Minerals Division National Institute for Interdisciplinary Science and Technology (CSIR), Trivandrum-695 019, India, and* §*Physikalisches Institut, Univerisität Stuttgart, Pfaffenwaldring 57, 70550 Stuttgart, Germany*

Received February 16, 2010. Revised Manuscript Received July 2, 2010

$Sr_{2-x}Ca_xMgTeO_6$ ($0 \le x \le 2$) ceramics were prepared by the solid-state ceramic route. Structure and microstructure of the compounds were investigated using XRD, TEM, and SEM methods. The system undergoes a transition from pseudocubic tetragonal $I4/m$ symmetry for $x = 0$ (Sr_2MgTeO_6) to pseudotetragonal monoclinic $P2_1/n$ symmetry for $x > 0$. The dielectric properties of the ceramics were studied by the resonance method. The temperature coefficient of resonant frequency is negative throughout the series; permittivities were in the range 13.2−14.3, and quality factors varied from 27 500 to 81 000 (5−6 GHz).

Introduction

The modern proliferation of wireless telecommunication technologies has increased the demand for low-loss microwave dielectric ceramics.[1−5] Even though a number of microwave resonator materials are available, the search for new materials with useful properties continues.[4,5] Extensive research has been carried out to investigate the properties of $A(B'_{1/3}B''_{2/3})O_3$ perovskites, like $Ba(Mg_{1/3}Ta_{2/3})O_3$ and $Ba(Zn_{1/3}Ta_{2/3})O_3$, as they possess an excellent combination of microwave dielectric properties;[6,7] however, less attention has traditionally been paid to microwave dielectric properties of $A(B'_{1/2}B''_{1/2})O_3$ double perovskites. Recent investigations by Khalam et al.[8,9] on these double perovskites showed a number of temperature-stable microwave dielectric compositions with relative permittivities greater than 20; however, because of a shortage of usable microwave frequency space, there is a push toward the millimeter-wave region (30−300 GHz).[10] To use dielectric resonators in this spectrum space, temperature-stable ceramics with $\varepsilon_r \approx 10$ are required.

Recently, tellurium-based dielectric ceramics showed excellent microwave properties with very low sintering temperatures (< 700 °C);[11−14] however, in most of these materials reported in the literature, Te exists in the 4^+ state. Bayer[15] reported the existence of new A_2MgTeO_6 (A = Sr, Pb, Ba) compounds in which Te is oxidized to the 6^+ state and which form stable perovskite structures in space group $Fm\bar{3}m$. More recently, Dias et al.[16] investigated the vibrational spectroscopic and microwave dielectric properties of A_2MgTeO_6 (A = Sr, Ba, Ca) ceramics. X-ray diffraction (XRD), Raman and infrared spectroscopic investigations of A_2MgTeO_6 (A = Sr, Ca) reported that the Sr-based compound was tetragonal, space group $I4/m$, and the Ca end member was monoclinic, space group $P2_1/n$.[16] The materials have low relative permittivities (11−14.3) and reasonably high quality factors (25 000−81 000). In the present study the crystal structure of $(Sr_{2-x}Ca_x)(MgTe)O_6$ ($0 \le x \le 2$) ceramics was investigated using transmission electron microscopy (TEM); and the microstructure and microwave dielectric properties are reported.

Experimental Methods

$Sr_{2-x}Ca_xMgTeO_6$ ($x = 0$, 0.5, 1, 1.5, 2) ceramics were prepared by a solid-state ceramic route. High purity $CaCO_3$, $SrCO_3$, and TeO_2 (99+%, Aldrich Chemical Co., Milwaukee, WI, USA)

*Corresponding author. Tel.: (208) 426 2309. Fax: (208) 426 2470. E-mail: RickUbic@BosieState.edu.

(1) Ubic, R.; Reaney, I. M.; Lee, W. E. *Int. Mater. Rev.* **1998**, *43*, 205.
(2) Sebastian, M. T. *Dielectric Materials for Wireless Communication*; Elsevier: Amsterdam, 2008, .
(3) Cava, R. J. *J. Mater. Chem.* **2001**, *11*, 54.
(4) Reaney, I. M.; Iddles, D. *J. Am. Ceram. Soc.* **2006**, *89*, 2063.
(5) Subodh, G.; James, J.; Sebasian, M. T.; Paniago, R.; Dias, A.; Moreira, R. L. *Chem. Mater.* **2007**, *19*, 4077.
(6) Nomura, S.; Toyama, K.; Kaneta, K. *Jpn. J. Appl. Phys.* **1982**, *21*, L624.
(7) Varma, M. R.; Resmi, R.; Sebastian, M. T. *Jpn. J. Appl. Phys.* **2005**, *44*, 298.
(8) Ohsato, H.; Tsunooka, T.; Sugiyama, T.; Kakimoto, K.; Ogawa, H. *J. Electro. Ceram.* **2006**, *17*, 445.
(9) Khalam, L. A.; Sebastian, M. T. *Int. J. Appl. Ceram. Technol.* **2006**, *3*, 364.
(10) Khalam, L. A.; Sebastian, M. T. *J. Am. Ceram. Soc.* **2007**, *90*, 1467.
(11) Subodh, G.; Sebastian, M. T. *J. Am. Ceram. Soc.* **2007**, *90*, 2266.
(12) Udovic, M.; Valant, M.; Suvrov, D. *J. Eur. Ceram. Soc.* **2001**, *21*, 1735.
(13) Kwon, D. K.; Lanagan, M. T.; Shrout, T. R. *J. Am. Ceram. Soc.* **2005**, *88*, 3419.
(14) Subodh, G.; Ratheesh, R.; Jacob, M. V.; Sebastian, M. T. *J. Mater. Res.* **2008**, *23*, 1551.
(15) Bayer, G. *J. Am. Ceram. Soc.* **1963**, *46*, 604.
(16) Dias, A.; Subodh, G.; Sebastian, M. T.; Lage, M. M.; Moreira, R. L. *Chem. Mater.* **2008**, *20*, 4347.

 Published on Web 07/27/2010

Table 1. Density, Microwave Dielectric Properties, and Tolerance Factors for $Sr_{2-x}Ca_xMgTeO_6$ ($0 \le x \le 2$) Ceramics Sintered at 1250 °C for 4 h

material	density (g/cm^3)	ε_r	ε_r (corrected)	Qf (GHz)	τ_f (ppm/°C)	t^a
Sr_2MgTeO_6	5.15 (90.7%)	14.3	14.8	27 500	−61	0.9914
$Sr_{1.5}Ca_{0.5}MgTeO_6$	5.34 (98.7%)	14	14.7	50 600	−66	0.9825
$SrCaMgTeO_6$	5.03 (98.4%)	13.8	14.6	57 100	−72	0.9736
$Sr_{0.5}Ca_{1.5}MgTeO_6$	4.76 (98.5%)	13.5	14.1	70 200	−77	0.9647
Ca_2MgTeO_6	4.24 (93.7%)	13.2	13.7	81 000	−81	0.9558

[a] t = tolerance factor (eq 1).

were used as the starting materials. Stoichiometric mixtures of powders were ball-milled in distilled water medium using yttria stabilized zirconia balls in a plastic container for 24 h. The slurry was dried then ground well and heated at a rate of 2.5 °C/min and kept at 700 °C for 4 h. A slow heating rate was used for the oxidation of Te^{4+} to Te^{6+}. The mixed powders were calcined at 1080 °C for 4 h. The calcined material was then ground into fine powder with a mortar and pestle and divided into different batches for sintering trials. $Sr_{2-x}Ca_xMgTeO_6$ ceramics have poor sinterability;[16] hence, 0.2 wt % B_2O_3 (Aldrich Chemical Co.) was added as a sintering aid and mixed thoroughly into the powders using distilled water. After drying, the powders were then mixed with 4 wt % PVA (average molecular weight 22,000, BDH Lab Suppliers, England) and again dried and ground by hand. Cylindrical pucks of about 10−11 mm height and about 20 mm diameter were made by applying a pressure of 150 MPa. These compacts were then fired at 600 °C for 30 min to expel the binder before sintering at temperatures ranging from 1175 to 1300 °C for 4 h. The bulk densities of the sintered samples were measured using Archimedes' method.

The crystal structure and phase purity of the powdered samples were studied by X- ray diffraction (XRD) using CuKα radiation (X'Pert MPD, PANalytical, Almelo, The Netherlands). High-resolution diffraction patterns were obtained from $10 \le 2\theta \le 130°$ using a step size of 0.008° and a dwell per step of 9.7 s. Lattice constants were calculated via La Bail refinements with the DIFFRACplus TOPAS 4.2 software package (Bruker AXS, Madison, WI).

The sintered samples were polished and then thermally etched for 18 min at 1150 °C, and the surface morphology was recorded by using a scanning electron microscope (S-4500, Hitachi High Technologies America, Inc., Pleasanton, CA, USA). Samples for transmission electron microscopy (TEM) were prepared by thinning pellets to electron transparency by conventional ceramographic techniques followed by ion thinning (PIPIS model 691, Gatan, Pleasanton, California, USA) to electron transparency for observation in the TEM (JEM-2100 HR, JEOL, Japan).

The microwave dielectric properties were measured by a vector network analyzer (8753 ET, Agilent Technologies). The dielectric constant and unloaded quality factor of samples were measured by the Hakki-Coleman[17] and cavity[18] methods (in the frequency range 4−6 GHz), respectively. The specimen was placed on a low-loss quartz spacer inside a copper cavity whose inner side was silver plated. The use of the low-loss single-crystal quartz spacer reduces the effect of losses due to the surface resistivity of the cavity. The diameter of the cavity was about 4 times larger than that of the sample for better isolation of the excited $TE_{01\delta}$ mode. The τ_f was measured by noting the variations of $TE_{01\delta}$ mode frequency with temperature in the range 25 to 75 °C.

(17) Hakki, B. W.; Coleman, P. D. *IEEE Trans. Microwave Theory Tech.* **1960**, *8*, 402.
(18) Krupka, J.; Derzakowski, K. D.; Riddle, B.; Jarvis, J. B. *Meas. Sci. Technol.* **1998**, *9*, 1751.

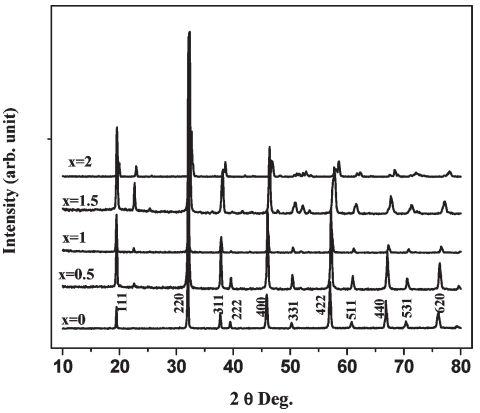

Figure 1. X-ray diffraction patterns of $Sr_{2-x}Ca_xMgTeO_6$ ($0 \le x \le 2$) ceramics sintered at 1250 °C/4 h. The indexing is according to the doubled pseudocubic unit cell.

Results and Discussion

Table 1 gives the density of 0.2 wt % B_2O_3 added $Sr_{2-x}Ca_xMgTeO_6$ ($x = 0, 0.5, 1, 1.5, 2$) ceramics. The sintering temperature of these ceramics is optimized at 1250 °C. The relative density was >98% ρ_{th} for $0.5 \le x \le 1.5$, but lower densities were achieved for $x = 2$ (93.7%) and $x = 0$ (90.7%). Figure 1 shows the XRD patterns of $Sr_{2-x}Ca_xMgTeO_6$ ($x = 0, 0.5, 1, 1.5, 2$) ceramics. The pseudocubic lattice constant varies from 3.95 Å (Sr_2MgTeO_6) to 3.85 Å (Ca_2MgTeO_6).

Figure 2 shows the microstructures of 0.2 wt % B_2O_3-added $Sr_{2-x}Ca_xMgTeO_6$ ($x = 0, 0.5, 1, 1.5, 2$) ceramics. The Sr_2MgTeO_6 sample ($x = 0$, Figure 2a) shows a distribution of grain sizes smaller than ~3 μm and an appreciable amount of fine intergranular porosity. The micrographs in Figure 2b−e show that the average grain size increases slightly with increasing Ca content, as does the scale of the porosity; however, no secondary phases were observed in any of the SEM micrographs, indicating the existence of a complete solid solution. The darker phase in Figure 2 is porosity.

Selected area electron diffraction patterns for Sr_2MgTeO_6, $Sr_{1.5}Ca_{0.5}MgTeO_6$, and Ca_2MgTeO_6 are shown in Figure 3, which summarizes the in-phase tilts of these perovskites. In each $\langle 100 \rangle_c$ pattern, a single set of γ superlattice reflections of the form $1/2\{\text{odd,odd,even}\}_c$ is possible. Each set would correspond to in-phase tilting of oxygen octahedra about a particular pseudocubic axis. In the case of $Sr_{1.5}Ca_{0.5}MgTeO_6$ and Ca_2MgTeO_6, γ reflections are only visible in the $[100]_c$ zone axis, indicating in-phase tilting about a single axis. The $\langle 111 \rangle_c$ patterns are a more succinct way of showing the same result in that each

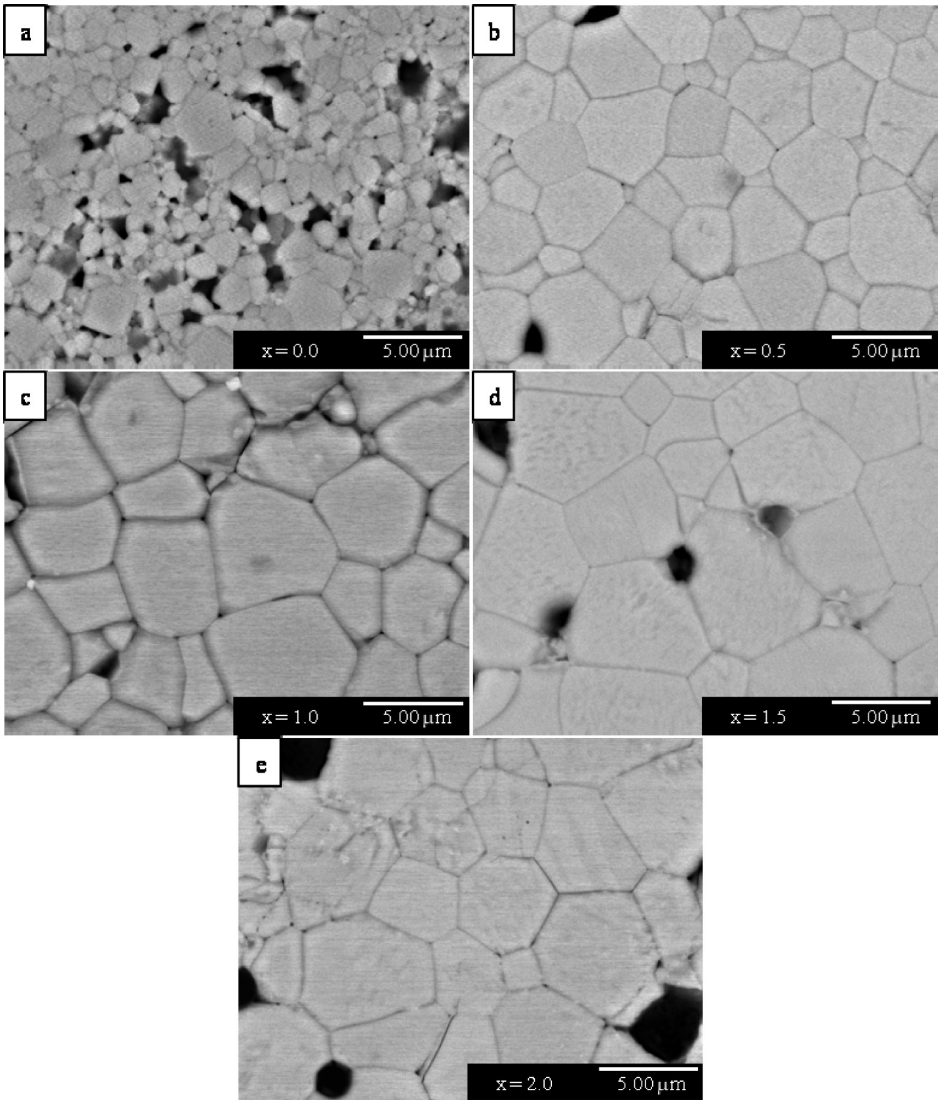

Figure 2. Backscattered SEM images showing the microstructures of $Sr_{2-x}Ca_xMgTeO_6$ ($0 \leq x \leq 2$) ceramics sintered at 1250 °C for 4 h and thermally etched: (a) $x = 0$, (b) $x = 0.5$, (c) $x = 1$, (d), $x = 1.5$, and (e) $x = 2$.

shows evidence of a single set of γ reflections, in this case 1/2{even,odd,odd} corresponding to in-phase tilting about the pseudocubic *a* axis. The β superlattice reflections are associated with antiparallel A-site cation displacements. In the case of Sr_2MgTeO_6, no β or γ reflections are observed, indicating the absence of both antiparallel Sr^{2+} displacements and in-phase tilting.

Figure 4 shows additional electron diffraction patterns for Sr_2MgTeO_6, $Sr_{1.5}Ca_{0.5}MgTeO_6$, and Ca_2MgTeO_6. Here, β reflections are interpreted as for Figure 3; however, $1/2\{odd,odd,odd\}_c$ superlattice reflections labeled as "α", which are visible in every pattern, have two possible interpretations. One explanation might be antiphase tilting of oxygen octahedra; however, the fairly strong intensity makes it doubtful that this phenomenon on its own could explain the existence of such reflections. The α reflections in $[110]_c$ patterns are of the type where $k \neq l$ and $h \neq l$, suggesting antiphase tilts about either pseudocubic *a* or *b*; however, as Figure 3 shows in-phase tilting about *a*, the correct interpretation of the α reflections must be antiphase tilting about pseudocubic *b*. Similarly, the α reflections in $[101]_c$ patterns are of the type where $k \neq l$ and $h \neq k$, suggesting antiphase tilts about either pseudocubic *a* or *c*. Again, because it is not possible to tilt octahedral both in-phase and antiphase about the same axis, the correct interpretation for these superlattice reflections must be antiphase tilting about the pseudocubic *c*. Finally, the α reflections in $[011]_c$ patterns are of the type where $h \neq l$ and $h \neq k$, suggesting antiphase tilts about either pseudocubic *b* or *c*, confirming the structure already deduced from $[110]_c$ and $[101]_c$ patterns.

A second explanation for the strength of these α reflections might be so-called rock-salt ordering of Mg^{2+} and Te^{6+} cations, resulting in cell doubling. The large radius difference between Mg^{2+} ($r = 0.72$ Å)[19] and Te^{6+} ($r = 0.56$ Å)[19] coupled with the substantial charge difference would combine to result in a large driving force for such ordering. This effect has previously been reported in $La_2(ZnTi)O_6$ perovskites,[20] in which strong α reflections

(19) Shannon, R. D. *Acta Crystallogr., Sect. A* **1976**, *A32*, 751.
(20) Ubic, R.; Hu, Y.; Abrahams, I. *Acta Crystallogr., Sect. B* **2006**, *62*, 521.

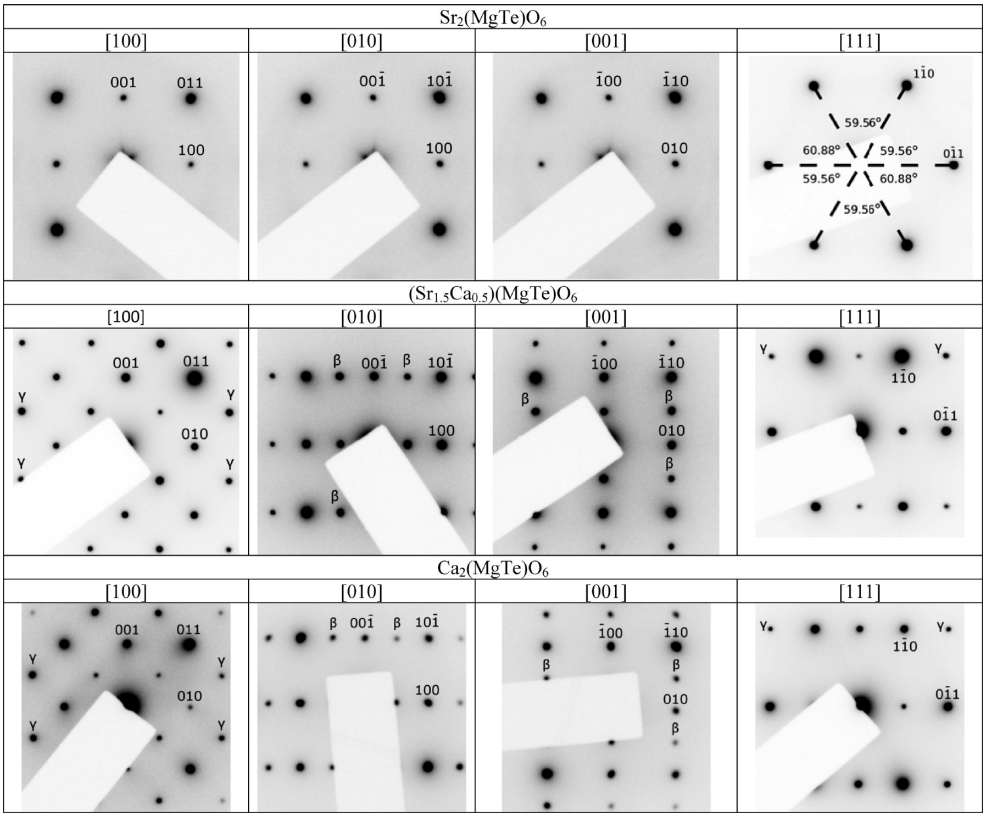

Figure 3. Electron diffraction patterns of $Sr_{2-x}Ca_xMgTeO_6$ ($x = 0$, 1.5, and 2) indexed according to the pseudocubic perovskite unit cell. Superlattice reflections are indicated as either β (beta) or γ (gamma) type.

are observed due to the combination of antiphase tilting and B-site cation ordering. A counter-example would be, for instance, the case of $(Sr_{0.8}Ce_{0.8})Ti_2O_6$,[21] where B-site ordering is not possible and α reflections are due only to antiphase tilting and so remain weak. The strength of the superlattice 111 peak in all the compositions shown in Figure 1 makes a further convincing case for B-site cation ordering. Although its very presence is insufficient to prove such ordering,[20] as antiphase octahedral tilting will make a small contribution to this peak, its consistent strength cannot be explained by octahedral tilting alone.

The stability of perovskite structures can be analyzed by means of the tolerance factor (t) as given in eq 1[22]

$$t = \frac{r_A + r_X}{\sqrt{2}(\langle r_B \rangle + r_X)} \quad (1)$$

where r_A and r_O are the ionic radii of the A-site cation and the anion, respectively; and $\langle r_B \rangle$ is the average ionic radius of the B-site cations. Several reports[23−27] are available in the literature correlating tolerance factor to temperature coefficient of resonance frequency. The relationship between τ_f and crystal structure in complex perovskite is complicated; however, Reaney et al.[25] provided an empirical relationship between τ_f (actually τ_ε, the temperature coefficient of permittivity, which is related to τ_f) and tolerance factor for many Nb- or Ta-based perovskite compounds. Their empirical relation between τ_f and tolerance factor shows three main regions, namely: $t < 0.965$, for which perovskites display both in-phase and antiphase tilts; $0.965 \leq t \leq 0.985$, for which only antiphase tilting is observed; and $t > 0.985$, for which perovskites are untilted.

Using Shannon's ionic radii data,[19] eq 1 shows that all the tolerance factors in the $Sr_{2-x}Ca_xMgTeO_6$ system are in the range of a stable perovskite ($0.9558 \leq t \leq 0.9914$). In particular, the average tolerance factor of Sr_2MgTeO_6 ($x = 0$) is $t = 0.9914$, close enough to unity to imply an untilted cubic structure. In this case, the α superlattice reflections visible in the electron diffraction patterns of Figure 3 corresponding to this composition can be interpreted as arising, not from octahedral tilting, but rather from ordering of Mg^{2+} and Te^{6+} on alternating {111} planes, resulting in a doubling of the cubic perovskite lattice constant ($a \approx 7.9$ Å) in space group $Fm\bar{3}m$, in agreement with previous work by Bayer.[15] In such a structure, Sr^{2+}, Mg^{2+}, Te^{6+}, and O^{2-} ions occupy 8c, 4b, 4a, and 24e sites, respectively; however, the tetragonal model in $I4/m$ ($a^0a^0c^-$) reported previously[16] cannot be ruled out on the strength of this evidence alone. While the closeness of the tolerance factor to unity ($t = 0.9914$) makes such a structure at first seem unlikely, it must be

(21) Ubic, R.; Subodh, G.; Sebastian, M. T.; Gout, D.; Proffen, T. *Ceram. Trans.* **2009**, *204*, 177.
(22) Goldschmidt, V. M. *Die Naturwiss.* **1926**, *14*, 477.
(23) Reaney, I. M.; Ubic, R. *Ferroelectrics* **1999**, *228*, 23.
(24) Colla, E. L.; Reaney, I. M.; Setter, N. *J. Appl. Phys.* **1993**, *74*, 3414.
(25) Reaney, I. M.; Colla, E. L.; Setter, N. *Jpn. J. Appl. Phys.* **1994**, *33*, 3984.
(26) Wise, P. L.; Reaney, I. M.; Lee, W. E. *J. Mater. Res.* **2002**, *17*, 2033.
(27) Reaney, I. M.; Wise, P. L.; Ubic, R.; Breeze, J.; Alford, N. McN.; Iddles, D.; Cannel, D.; Price, T. *Philos. Mag.* **2001**, *A81*, 501.

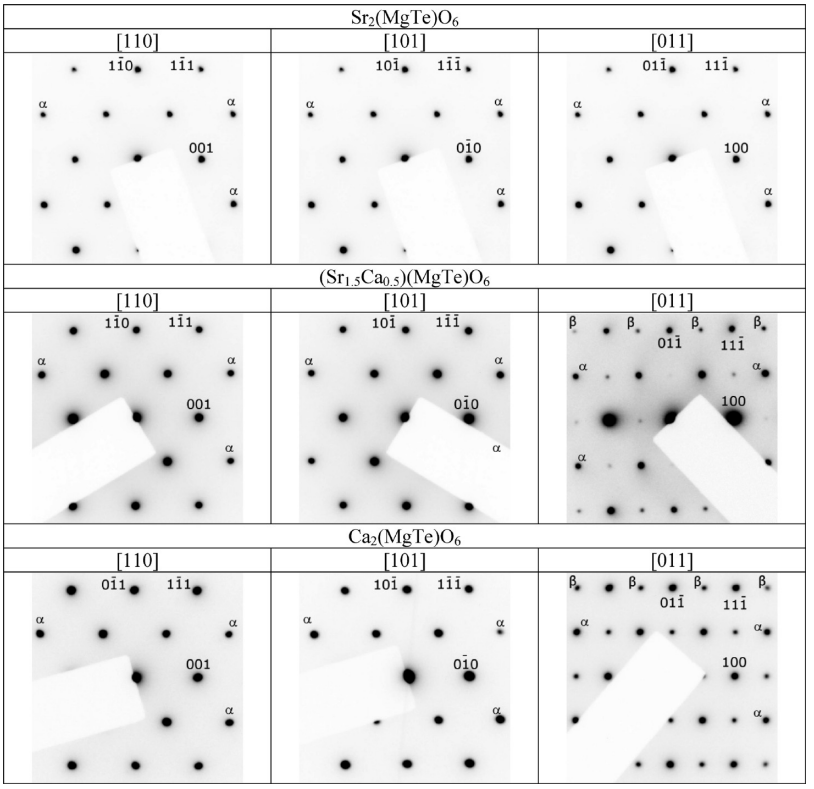

Figure 4. Electron diffraction patterns of $Sr_{2-x}Ca_xMgTeO_6$ (x = 0, 1.5, and 2) indexed according to the pseudocubic perovskite unit cell. Superlattice reflections are indicated as either β (beta) or α (alpha) type.

remembered that there is no real "average" tolerance factor. Each perovskite unit will contain either Mg^{2+} or Te^{6+}, and thus have a tolerance factor of either 0.9531 (B = Mg^{2+}) or 1.0329 (B = Te^{6+}). In this case, it seems reasonable to argue that the low tolerance factor caused by Mg^{2+} on the B site (unusual for an oxide perovskite) is sufficient to cause the tilting observed experimentally. In addition, there are several reports of ceramics with simultaneously high tolerance factors and tilted structures in $I4/m$, including Sr_2FeMoO_6 (t = 0.9976)[28] and Sr_2CrTaO_6 (t = 0.9976).[29] In this case, α superlattice reflections would occur in every $\langle 110\rangle_c$ zone axis, not just because of tilting ($a^0a^0c^-$), but because of B-site ordering as well. The additional possibilities that tilting is present, not just about one axis, but about two, as in the monoclinic space group $C2/m$ ($a^0b^-b^-$), or even all three, as in rhombohedral $R\bar{3}$ ($a^-a^-a^-$), must also be considered; however, on close inspection, neither the $\langle 100\rangle_c$ patterns, which do not contain 001_m (β) reflections allowed in $C2/m$, or the $\langle 110\rangle_c$ patterns, which contain several reflections forbidden in $C2/m$, can be explained in this symmetry. Similarly, the $[111]_c$ pattern, which would correspond to the [001] axis in the trigonal $R\bar{3}$ ($a^-a^-a^-$) model or [111] in the cubic $Fm\bar{3}m$ ($a^0a^0a^0$) model, should display 3-fold symmetry in either of these models; however, on close inspection, the lack of such symmetry becomes apparent. Instead of equal angles of 60°, angles of between 59.6° and 60.9° are observed (Figure 3), suggesting a tetragonality of $c/a \approx 1.45$. The tetragonal description of the ideal perovskite structure would yield $c/a = \sqrt{2} \approx 1.41$. Furthermore, the splitting previously observed[16] in XRD data makes the cubic $Fm\bar{3}m$ structure unlikely. The only structural possibility which seems to remain is $I4/m$ ($a^0a^0c^-$), with ordering on the B site and antiphase tilting about a single axis presumably stabilized by the large Mg^{2+} ion. As the tetragonal distortion is small, the structure can still be accurately

Table 2. Lattice Constants $Sr_{2-x}Ca_xMgTeO_6$ ($0 \le x \le 2$) Ceramics

material	structure	a (Å)	b (Å)	c (Å)	β (deg)
Sr_2MgTeO_6	$I4/m$	5.5909(1)	5.5901(2)	7.9251(2)	90
$Sr_{1.5}Ca_{0.5}MgTeO_6$	$P2_1/n$	7.8906(2)	5.5708(2)	5.5735(2)	89.849(3)
$SrCaMgTeO_6$	$P2_1/n$	7.9113(2)	5.5561(1)	5.5528(8)	89.700(2)
$Sr_{0.5}Ca_{1.5}MgTeO_6$	$P2_1/n$	7.9184(2)	5.5324(2)	5.5177(2)	89.52(3)
Ca_2MgTeO_6	$P2_1/n$	7.9249(3)	5.5289(3)	5.4950(2)	89.07(3)

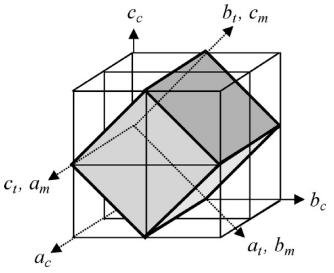

Figure 5. Schematic diagram of the relationship between the cubic (ideal), tetragonal (x = 0), and monoclinic ($0.5 \le x \le 2$) perovskite unit cells. One tetragonal/monoclinic unit cell is inscribed inside eight primitive cubic unit cells. The subscripts correspond to the three different crystal classes.

(28) Chmaissem, O.; Kruk, R.; Dabrowski, B.; Brown, D. E.; Xiong, X.; Kolesnik, S.; Jorgensen, J. D.; Kimball, C. W. *Phys. Rev.* **2000**, *B62*, 14197.
(29) Barnes, P. W.; Lufaso, M. W.; Woodward, P. M. *Acta Crystallogr., Sect. B* **2006**, *62*, 384.

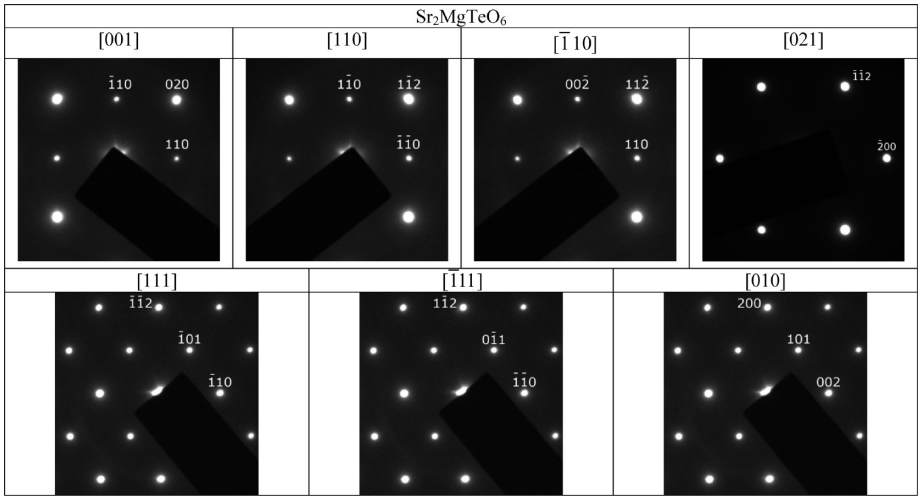

Figure 6. Electron diffraction patterns of Sr_2MgTeO_6 from Figures 3 and 4 reindexed according to the model in $I4/m$.

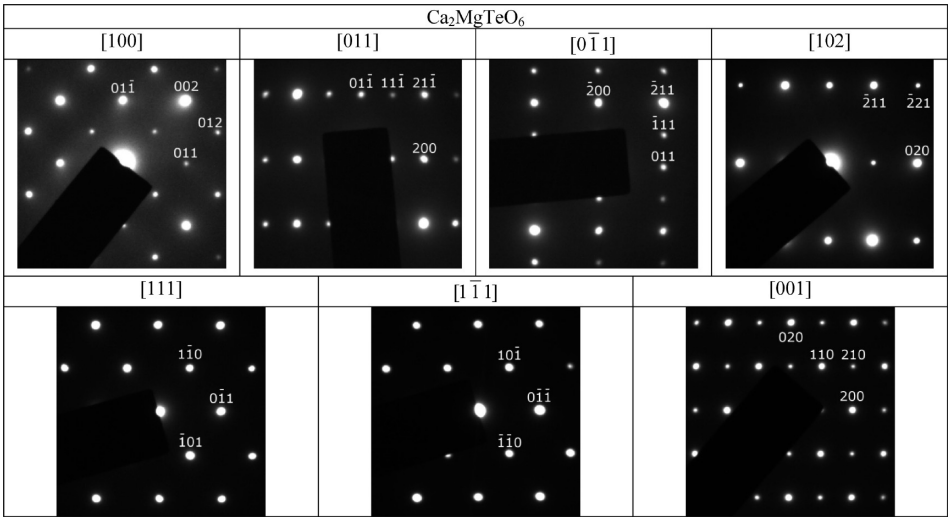

Figure 7. Electron diffraction patterns of Ca_2MgTeO_6 from Figures 3 and 4 reindexed according to the model in $P2_1/n$.

described as pseudocubic. The refined lattice constants are $a = b = 5.5909(1)$ Å, $c = 7.9251(2)$ Å. The equivalent pseudocubic lattice constant is $a_{pc} = 3.9564$ Å.

The tolerance factors for $x = 0.5$ ($t = 0.9825$) and $x = 1$ ($t = 0.9736$) compositions would imply the existence of antiphase tilting of oxygen octahedra; however, Figure 3 also shows the existence of γ reflections corresponding to in-phase tilting as well. In fact, these patterns are more or less identical to the ones observed for $x = 1.5$ ($t = 0.9647$) and $x = 2$ ($t = 0.9558$) compositions, the lower tolerance factors of which support the existence of both in-phase and antiphase tilts of oxygen octahedra and consequent lowering of symmetry, in agreement with Figure 3. The possible tilt systems are $a^+b^-c^-$, $a^+a^-c^-$, $a^+b^-b^-$ and $a^+a^-a^-$; however, Howard et al. [30] showed by a group theoretical approach that, in fact, the $a^+b^-c^-$, $a^+a^-c^-$, and $a^+a^-a^-$ tilt systems cannot be produced by octahedral tilting or cation ordering, leaving just $a^+b^-b^-$, corresponding to *Pmnb* symmetry[31] or $P2_1/n$.[30] As B-site ordering is not possible in the orthorhombic *Pmnb* space group, a monoclinic structure in $P2_1/n$ (a maximal nonisomorphic subgroup of *Pmnb*) is the only choice, which seems to explain all the observed phenomena in these compositions. The results of Le Bail refinements are shown in Table 2. As the distortion is again quite small ($b \approx c, \beta \approx 90°$), all these compositions can be described as pseudotetragonal. As it happens, in their review of more than 160 ordered double perovskite oxides, Anderson et al.[32] noted that the most commonly occurring structures were those in $Fm\bar{3}m$ (tilt system $a^0a^0a^0$) and $P2_1/n$ (tilt system $a^+b^-b^-$).

Models of both the tetragonal structure of Sr_2MgTeO_6 and the monoclinic structure of $Sr_{2-x}Ca_xMgTeO_6$ ($0.5 \leq x \leq 2$) are compared to the ideal cubic perovskite unit cell in Figure 5. The tetragonal cell is shown in the conventional orientation with the unique axis on c, whereas the monoclinic one is shown in the orientation used by Glazer[31] for perovskites in the $a^+b^-b^-$ tilt system. The electron diffraction patterns of Figures 3-4 can now be reinterpreted according to models in either $I4/m$ ($x = 0$) or $P2_1/n$

(30) Howard, C. J.; Kennedy, B. J.; Woodward, P. M. *Acta Crystallogr., Sect. B* **2003**, *59*, 463.
(31) Glazer, A. M. *Acta Crystallogr., Sect. A* **1975**, *31*, 756.
(32) Anderson, M. T.; Greenwood, K. B.; Taylor, G. A.; Poeppelmeir, K. R. *Prog. Solid State Chem.* **1993**, *22*, 197.

($0.5 \leq x \leq 2$) and the resulting indexing is shown schematically in Figures 6-7. The phase transition can be thought of as proceeding from pseudocubic Sr_2MgTeO_6 to pseudotetragonal $Sr_{2-x}Ca_xMgTeO_6$ ($0.5 \leq x \leq 2$), with the degree of distortion increasing with x.

All materials in the $Sr_{2-x}Ca_xMgTeO_6$ ($x = 0, 0.5, 1, 1.5, 2$) system show optimal microwave properties on sintering at 1250 °C for 4 h, as summarized in Table 1. The permittivity decreases as x increases (increasing Ca content) while the quality factor increases. Although the samples were all fairly dense, a small correction for the effect of porosity on permittivity values was applied using the Bötcher mixing rule,[33] which, at such low porosity levels, happens to agree exactly with the older and more familiar Maxwell-Garnett approximation.[34] A systematic decrease in τ_f from −61 ppm/°C at $x = 0$ (Sr_2MgTeO_6) to −81 ppm/°C at $x = 2$ (Ca_2MgTeO_6) was also observed. Given the tilted nature of the corresponding compounds, this decrease is in accordance with the general trend observed by Reaney et al.[25]

(33) Bötcher, C. J. F. J. R. Neth. Chem. Soc. **1945**, *64* 47.
(34) Maxwell-Garnett, J. C. *Philos. Trans. R. Soc. London, Ser. A* **1904**, *203*, 385.

Conclusions

$Sr_{2-x}Ca_xMgTeO_6$ ceramics have been fabricated to near full density and their crystal structures investigated via XRD and electron diffraction. On the basis of the observed symmetries and superlattice reflections in electron diffraction patterns, there is a phase transition from a pseudocubic tetragonal $I4/m$ structure for the $x = 0$ end member (Sr_2MgTeO_6) to a pseudotetragonal monoclinic $P2_1/n$ structure for $x \geq 0.5$. The low symmetries and tilted structures, despite relatively high tolerance factors for $x \leq 1$, have precedents in the literature and are probably the result of the sharing of B sites with relatively large Mg^{2+} ions. The average grain size increases slightly with increasing Ca content. The dielectric constant gradually decreases from 14.3 at $x = 0$ to to 13.2 at $x = 2$, whereas the Qf values simultaneously increase from 27 500 to 81 000 and τ_f decreases from −61 ppm/°C to −81 ppm/°C.

Acknowledgment. This work has been supported by the National Science Foundation's Major Research Instrumentation Program, Award 0521315 and 0619795. G. Subodh also acknowledges the AvH foundation for financial support.